First applications of the ICRF modelling code PION in the ITER Integrated Modelling and Analysis Suite

I.L. Arbina[1], M.J. Mantsinen[1,2], X. Sáez[1], D. Gallart[1], A. Gutiérrez[1], D. Taylor[3], T. Johnson[4], S.D. Pinches[5], M. Schneider[5] and the EUROfusion-IM Team*

[1]*Barcelona Supercomputer Center (BSC), Barcelona, Spain*
[2]*ICREA, Barcelona, Spain*
[3]*CCFE, Culham Science Centre, Abingdon, Oxon, OX14 3DB, UK*
[4]*KTH Royal Institude of Technology, Stockholm, Sweden*
[5]*ITER Organization, Route de Vinon-sur-Verdon, CS 90 046, 13067 St Paul-lez-Durance Cedex, France;*
**http://www.euro-fusionscipub.org/eu-im*

Introduction Ion Cyclotron Range of Frequency (ICRF) heating is one of the three auxiliary heating methods foreseen for ITER. The ICRF scenarios in the ITER non-activated phase have been recently reassessed with emphasis on the heating and current drive performance and H-mode access based on the calculation of the core single pass absorption (SPA) [1]. In this work we study these ICRF scenarios using the ICRF modelling code PION [2]. The PION code computes the time evoluton of the ICRF power absorption and the distribution functions of the resonant ions in a self-consistent way. It has been extensively compared against experimental results for a large variety of ICRF schemes on JET, AUG, DIII-D and Tore Supra. It is based on simplified models, which makes it relatively fast and, thereby, suitable for use in an integrated modelling framework such as the ITER Integrated Modelling and Analysis Suite (IMAS) [3]. The results reported here are the first applications of PION integrated in IMAS.

ICRF heating scenarios in ITER non-activated phase We focus on a number of ICRF scenarios with SPA greater than 0.5 as identified in [1]. We use the steady-state equilibrium and core profiles provided by the transport code METIS [4] in the ITER IMAS Scenarios Database. Table I shows the scenarios considered. They include:

- Cases T.a and T.b in H plasmas with different plasma density and case T.c in ^{4}He plasmas, all with second harmonic heating of H at one third of the full magnetic field (third-field).
- Four cases with H minority heating (H.a-H.d) for one half of the full magnetic field (half-field) in ^{4}He plasmas for different H minority ion concentrations.
- Three-ion ICRF scenario [5] (F.a) in a H plasma with 17% ^{4}He mixture and 0.1% ^{3}He at the full-field.

The magnetic field B_0 has been adjusted to have a central resonance, the ICRF power is 10 MW and a single toroidal mode number $N = 32$ is considered.

Table II summarizes our results. They include the power absorbed by the main resonant ion species P_{abs}, the fraction of the total collisional power transferred by the main resonant ions to bulk ions and electrons $P_{\mathrm{ci}}/P_{\mathrm{c}}$ and $P_{\mathrm{ce}}/P_{\mathrm{c}}$, respectively, and the ICRF-enhancement of the total and parallel energy content of the main resonant ions ΔW and $\Delta W_{\|}$, respectively. The ICRF power absorbed by the rest of the resonant ions species is below 1% of the total ICRF power and the remaining ICRF power is damped by electrons. In Table II we also show the perpendicular wave number $k_{\perp}$ and the ratio of right (E_-) and left (E_+) hand polarized electric fields, $|E_-/E_+|$,

Table I. Parameters for the third-field (T), half-field (H) and full-field (F) cases considered. Here METIS Shot-Run are listed, B_0 is the magnetic field at the magnetic axis, f is the frequency of the wave, n_e is the electron density, T_e and T_i are the electron and ion temperature, respectively, and n_G is the Greenwald density. The concentrations are given with respect to n_e. For half-field cases H.a-d, the H concentrations are 1, 2, 5, 9.2%, respectively.

Case	Shot-Run	Main ion	Scheme	B_0 (T)	f (MHz)	$n_e \times 10^{19}$ (m^{-3})	T_e (keV)	T_i (keV)	Comments
T.a	100014-1	H	$2\omega_{cH}$	1.74	53	2.4	17.4	7.0	$n_e = 0.5\, n_G$
T.b	100015-1	H	$2\omega_{cH}$	1.74	53	4.3	10.5	5.8	$n_e = 0.9\, n_G$
T.c	110015-1	^{4}He	$2\omega_{cH}$	1.74	53	1.9	15.4	8.2	5% H
H.a-d	110005-1	^{4}He	ω_{cH}	2.62	40	3.3	10.2	10.9	1,2,5,9.2% H
F.a	100001-1	H	ω_{c^3He}	5.2	53	5.6	8.4	9.7	0.1%^{3}He, 17%^{4}He

Table II. Results of PION simulations for cases in Table I.

Case	ΔW (MJ)	$\Delta W_{\parallel}$ (MJ)	P_{abs} (MW)	P_{ci}/P_c (%)	P_{ce}/P_c (%)	$k_\perp$ (m^{-1})	$\lvert E_-/E_+\rvert$	E_{crit} (keV)	$\langle E_{fast}\rangle$ (MeV)
T.a	3.0	0.11	7.3	45	55	38.7	4.9	250	0.7
T.b	0.6	0.05	8.2	72	28	53.7	3.6	150	0.13
T.c	4.0	0.21	4.8	13	87	51.3	1.8	140	1.4
H.a	3.0	0.08	6.2	10	90	33.9	3.5	90	5.5
H.b	3.5	0.12	7.7	12	88	34.0	3.4	92	4.8
H.c	3.7	0.37	8.0	25	75	31.9	4.2	96	4.1
H.d	3.7	0.55	7.9	38	62	30.0	6.1	101	2.7
F.a	1.0	0.02	9.6	32	68	11.0	0.4	443	1.5

at the resonance, as well as the critical energy $E_{crit} = 14.8 A T_e \left[\sum_i n_s Z_i^2/(n_e A_i)\right]^{2/3}$ [6] and an estimation of the average maximum energy $\langle E_{fast}\rangle$ of main resonating ions. Here, the sum is over the thermal ion species i. We discuss each case in more detail below.

► **Third-field** For the third-field the wave frequency is tuned to match the hydrogen second harmonic resonance on-axis. For H plasmas (T.a and T.b), table II shows that the resonant hydrogen absorbs 73% of the wave power in the case with lower density (T.a) and 82% in the case with higher density. The fraction of the collisional power transferred to ions and electrons with respect to the total collisional power shows that electron heating dominates over ion heating in T.a case while bulk ion heating dominates in T.b case. This difference is because the formation of a high-energy tail in the distribution function of the resonant ions is stronger in case T.a and, consequently, the critical energy of the resonating species of case T.a fulfils $(E_{crit})_{T.a} < \langle E_{fast}\rangle_{T.a}$, leading to Coulomb collisions with the background electrons. In case T.b $(E_{crit})_{T.b} > \langle E_{fast}\rangle_{T.b}$, favouring the collisions of the resonant species with the thermal ions. Figures 1b and 1d show the corresponding collisional power density as a function of the normalized flux surface s. Figures 1a and 1c show the radial profiles of the absorbed power density for the thermal plasma (t_i) and in the steady-state (t_f). We can see that the most of the ICRF power is deposited centrally within $s < 0.4$. Finite orbit effects widen and flatten the absorption density profile from the thermal plasma to its steady-sate. The finite orbit width effects are stronger in the case with lower density, as expected.

In the case of ^{4}He plasma at third-field (T.c), the heating scheme is the same as in H plasmas at third-field but H is now a minority ion species. We have assumed a H concentration of 5% of electron density. In this case as compared to cases T.a and T.b, PION predicts that H absorption is weaker, i.e. 48% of the total ICRF power. Nevertheless, a high-energy tail is generated in

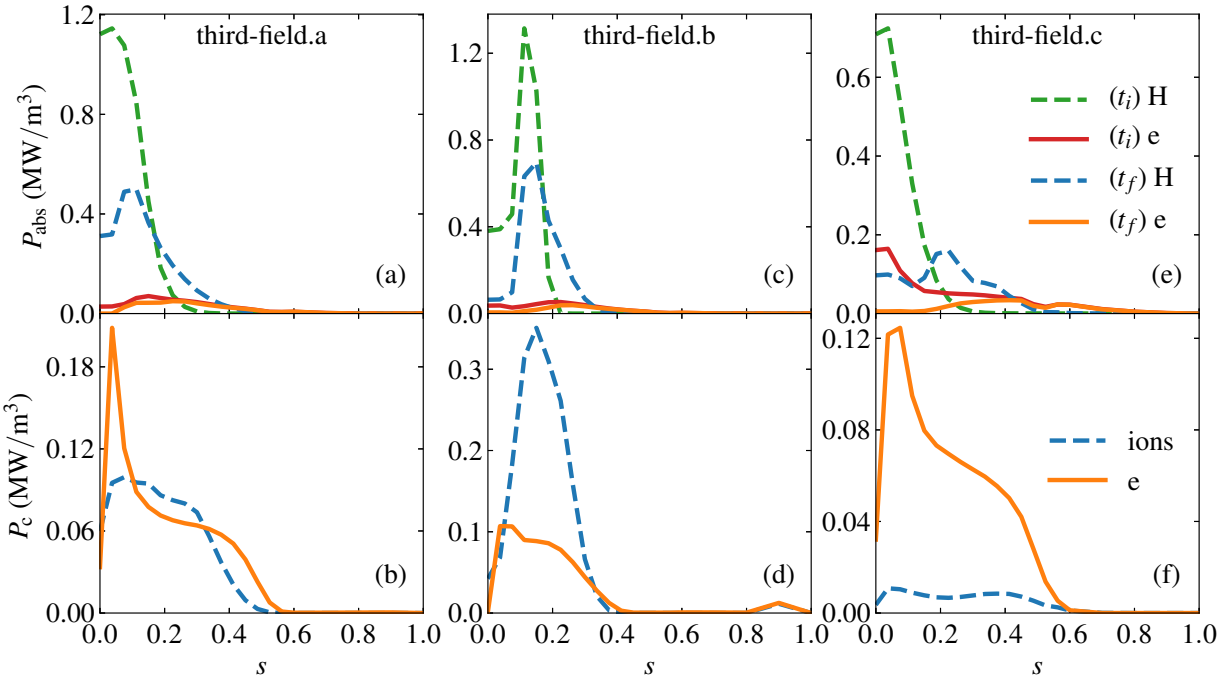

Figure 1. (Top) RF-power density absorbed by the resonant ion species (dashed), H, and the electrons (solid) as a function fo the normalized flux surface, s, for the different cases at one third of the field for the thermal plasma (t_i) and steady-state (t_f). (Bottom) Power density transferred from the resonant ions to the background electrons and ions through collisions as a function of the normalized flux surface, s, in the steady-state.

the distribution function of resonant H ions. Since $(E_{\text{crit}})_{\text{T.c}} \ll \langle E_{\text{fast}} \rangle_{\text{T.c}}$, most of the absorbed power is transferred to the electrons. Figures 1e and 1f show the effects of these high-energy fast ions in the broadening and flattening of the radial profile of the absorbed power density and collisional transferred power density profile as compared to the initial H absorption profile (green curve labelled t_i in Fig. 1e).

► **Half-field** For the half-field cases H.a-d, the wave frequency is set to 40 MHz, tuned to the fundamental H resonance on-axis. In table II we see that the power absorption of the resonant ion species increases with the concentration until 5% H, where is reaches its maximum, in overall agreement with the results reported in [7]. For all half-field cases H damping gives rise to formation of a high-energy tail in the resonating ions distribution function with $(E_{\text{crit}})_{\text{H}} < \langle E_{\text{fast}} \rangle_{\text{H}}$. This explains the predominance of electron heating, as can be seen in Fig. 2b for the 5% H minority. The ratio $P_{\text{ci}}/P_{\text{c}}$ increases with increasing minority concentration indicating that bulk ion heating becomes more dominant for increasing concentration of the minority species. Figure 2a shows the absorbed power density profile of 5% H concentration case showing a similar behaviour as in T.a and T.c cases, with finite orbit width effects widening and flattening the radial profiles.

► **Full-field** For the full-field case F.a the wave frequency is $f = 53$ MHz, tuned to resonate with fundamental ^{3}He on-axis. This case presents the so-called three-ion scheme for H-^{4}He ion-species mixture with ^{3}He minority ions. Table II shows that the power absorption of the resonating ions, 96%, is maximum in comparison with all the other cases studied. The fact that $|E_+| > |E_-|$ in this case favours the ion absorption of ICRF power. High-energy fast ions are created in this scenario. Since $(E_{\text{crit}})_{\text{F.a}} < \langle E_{\text{fast}} \rangle_{\text{F.a}}$ collisional transfer power density mainly

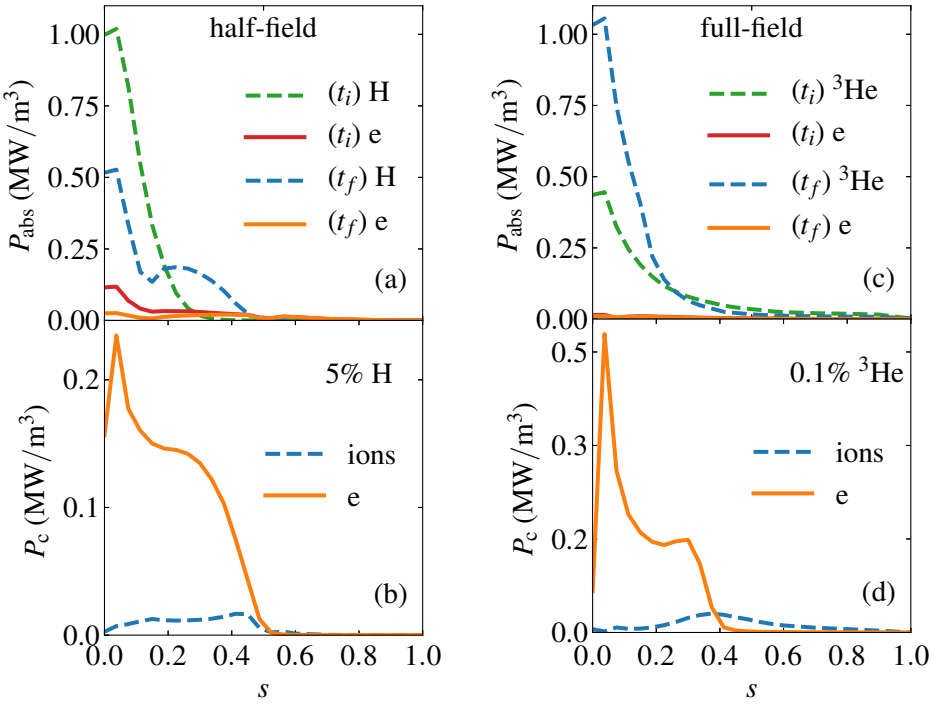

Figure 2. As in Fig. 1 but for the half-field case H.c with 5% H minority (left) and the full-field three-ion case F.a with 0.1% ^{3}He minority (right).

goes to heat the background electrons as shown in Fig. 2d.

Conclusions We have presented results from first applications of the PION code in the ITER non-activated phase scenarios using the ITER IMAS infrastructure.

PION simulations on the ITER ICRF heating scenarios predict central heating of the main resonant ion species. The results show that most of the heating scenarios predict a dominance of bulk electron heating over thermal ion heating. Finite orbit width effects are appreciable, widening the resulting power deposition over a wide radial region.

For the full-field with the three-ion scheme in a H-^{4}He mixture plasma with ^{3}He minority, PION predicts stronger power absorption of the resonant ions with respect the other cases studied due to the enhanced wave field $|E_+| > |E_-|$ at the resonance. For the assumed low ^{3}He concentration of 0.1% with respect to the electron density, the resonant ^{3}He minority provide mainly collisional electron heating.

Acknowledgements This work has been carried out within the framework of the EUROfusion Consortium and has received funding from the Euratom research and training programme 2014-2018 and 2019-2020 under grant agreement No 633053. The views and opinions expressed herein do not necessarily reflect those of the European Commission or the ITER Organization.

References

[1] M. Schneider *et al.*, EPJ Web. Conf. 157, 03046 (2017)
[2] L.-G. Eriksson *et al.*, Nucl. Fusion **33**, 1037 (1993)
[3] F. Imbeaux *et al.*, Nucl. Fusion **55**, 123006 (2015)
[4] J. F. Artaud *et al.*, Nucl. Fusion **50**, 043001
[5] Ye. O. Kazakov *et al.*, 45th EPS Conf. on Plasma Physics, P5.1047 (2018)
[6] T. H. Stix, Plasma Physics **14** 367 (1972)
[7] R. Bilato *et al.*, AIP Conf. 1580, 291-294 (2014)